Design of a Permanent Magnet Electric Variable Transmission for HEV Applications

Yuan Cheng[1,4,5], Christophe Espanet[1,5], Rochdi Trigui[2,5], Alain Bouscayrol[3,5], Shumei Cui[4]
[1] FEMTO-ST Institute, ENISYS Dept., University of Franche-Comte, Belfort, France
[2] LTE, INRETS, Lyon, France
[3] L2EP, University of Lille 1, Lille, France
[4] Dept. Electrical Engineering, Harbin Institute of Technology, Harbin, China
[5] MEGEVH, French National Network on HEVs, France, **http://www.univ-lille1.fr/megevh**
Email: chengyuan@hit.edu.cn

***Abstract*-This paper focuses on a permanent magnet (PM) machine based electric variable transmission (PM-EVT) for HEV applications. The basic idea of EVT is firstly given as well as a state-of-the-art. To choose an appropriate PM-EVT structure, a detailed description of possible architectures is presented and the specifications are defined based on the well-known Toyota Prius hybrid car. Main design procedure and equations are presented. The first design is finished, some preliminary results are given.**

***Keywords*-hybrid electric vehicle; electric variable transmission; permanent magnet machine**

I. INTRODUCTION

The growing concerns about environment protection and global warming have accelerated the development of hybrid electric vehicles (HEVs) globally. By coupling the electric power systems (electric machines) with the conventional mechanical power systems (internal combustion engine, ICE), HEVs provide an alternative electric power flow in addition to the mechanic one and create additional degrees of freedom in the energy management of the vehicle. In this sense, HEVs make the power flows more efficient and produce less emission. The way and level of power coupling are key points of HEVs. Various novel HEV topologies could be found according to different coupling ways and levels [1]. This paper will present a novel HEV powertrain, named electric variable transmission (EVT), as an alternative solution to classical architectures.

The basic idea of EVT is illustrated in Fig.1. Interfacing multi-energy sources, EVT continuously achieves a contactless power transmission between mechanic sources (MS1 and MS2). Meanwhile, the introduction of an electric source (ES) offers a possibility of maximizing the system efficiency and minimizing the emissions by freely changing its input and output speeds and/or torques. Therefore, EVT is by essence a hybrid system, and has attracted increasing interests during last 5 years [2]-[10].

This paper is organized as follows: in Section II, the state-of-the-art of EVT will be reviewed as well as a description about choosing an appropriate permanent magnet EVT (PM-EVT) structure. To design such a PM-EVT, the specifications are defined in Section III based on the Toyota Prius hybrid car simulation. Main procedure and equations concerning PM-EVT design are presented in Section IV, and preliminary results are also given.

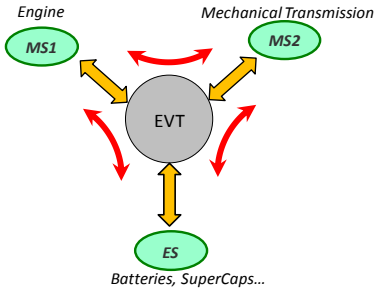

Fig. 1 The basic idea of EVT

II. STATE-OF-THE-ART AND CHOICE OF PM-EVT STRUCTURE

A. State-of-the-art

EVT concept and name were firstly presented by Prof. Hoeijmakers in 2004 [2]. It comes from a basic idea of replacing the conventional vehicle powertrain, including clutch, gearbox, starter and generator by only one electromechanical system. A prototype has been realized by using two concentrically arranged induction machines [3]. However, such a topology has a somewhat complex field distribution and leads to control difficulties. Besides, the efficiency is also a key factor for its application in vehicles [4]. Conceptually, various machine types can be applied into EVT instead of induction machine. Similar designs could be found by using PM brushless machines, reluctance machines and even DC machines [5]-[9]. For example, a four quadrant transducer (4QT) is studied in [5]: it has the similar structure than the one proposed in [2] except that it consists of two PM synchronous machines (PMSM). The dual mechanical ports machine (DMPM) is also a PM machine based EVT but the PM arrangement is different on its outer rotor [6]. Compound structure machines with radial-axial field or more complex structures are also studied in order to reduce the effect of field coupling or to enhance the machine performances [10].

Despite different names and principles, these electromechanical systems implement a continuous variation of gear ratio and a contactless power transmission by electrically regulating its input and output speeds and/or torques. Some common theory and application issues are being studied in order to promote the EVT technology including [11]:

- Modeling and field decoupling control
- Machine design and optimization
- Thermal analysis and cooling design

978-1-4244-8218-4/10/$26.00 ©2010 IEEE

- Reliability improvement
- Development of energy management strategy for EVT

In addition to the application in HEVs, some novel application fields, such as underwater propulsion and wind power generation system using the idea of EVT can also be found recently [12][13].

It can be seen from the overview of EVT researches that PM-EVT is becoming more attractive than other machine types. It does make sense because PM machines have the inherent merits of a higher efficiency and torque density and already became the most promising machines of modern EVs and HEVs [14][15]. Moreover, the use of PMs in the EVT leads to various topologies as well as interesting problematics of machine design and control. In this context, this paper will focus on PM-EVT: firstly the choice of structure and secondly the design.

B. Choice of PM-EVT Structure

The EVT concept needs at least the use of two electromechanical converters, electric machines (EM) typically, and two power electronic converters (PE). By controlling speed and torque of the electrical machines, the contactless power transmission between MS1 and MS2 is achieved. Although some EVT designs are realized with the aid of mechanical gearboxes, a combination of electric machines is simply considered in this paper.

Such an idea can be firstly implemented by referring to the architecture of series HEV (SHEV) illustrated in Fig.2 (a). The engine power is converted into electrical power through Shaft 1 and by using EM1. Then the electrical power is converted to mechanical energy again using EM2 in order to propel the vehicle through Shaft 2. Despite the advantages of simplicity and flexibility, it suffers greatly from the low transmission efficiency due to the fact that all the power is converted many times before it finally propels the vehicle. Another disadvantage is that EM1 and EM2 need to be sized for the maximum sustained power to satisfy the requirements of climbing a long grade [1].

In this scheme, we notice that the electromagnetic force is only used to fulfill the electromechanical conversion. The system efficiency will be increased and the sizes of EM1 and EM2 are also reduced greatly if the electromagnetic force could also be used to transfer the engine power, as in Fig.2 (b). In the second scheme, EM1 or EM2 must be a double rotor machine, so that two rotating parts are consequently allowable. The other machine should be a normal machine with one stator and one rotor. In this paper, it is assumed that EM1 is a double-rotor machine, and EM2 is a normal machine.

The engine power is converted into the electric part in EM1 and the direct traction part, the latter directly propels

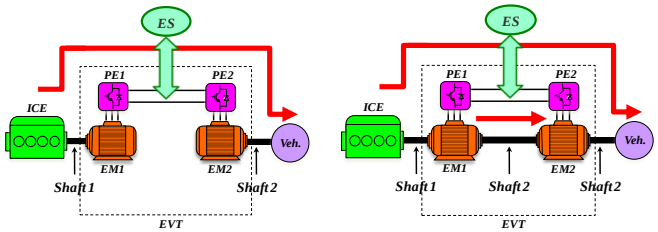

(a) Series HEV with EVT (b) Series-parallel HEV with EVT

Fig. 2 The HEVs with EVT

TABLE I
FOUR POSSIBLE ARCHITECTURES OF EM1

	OR connected to EM2, ***IR*** connected to Engine		***OR*** connected to Engine, ***IR*** connected to EM2	
	OR+IR= PM+W	***OR+IR= W+PM***	***OR+IR= PM+W***	***OR+IR= W+PM***
Easier & Better Cooling	No	No	No	No
Inertia on ICE shaft	Big	Small	Big	Big
Slip ring	Yes	Yes	Yes	Yes
Magnet bandage	No	Yes	No	Yes
Structure	complex	complex	complex	complex
	Arch. I	**Arch. II**	**Arch. III**	**Arch. IV**

TABLE II
FOUR POSSIBLE ARCHITECTURES OF EM2

	Structure of Outer Stator(**OS**)		Structure of Inner Stator(**IS**)	
	OS+Rotor= W+PM	***OS+Rotor= PM+W***	***IS+Rotor= PM+W***	***IS+Rotor= W+PM***
Easier & Better Cooling	Yes	No	No	Yes
Inertia on ICE shaft	Small	Big	Big	Big
Slip ring	No	Yes	Yes	No
Magnet bandage	Yes	No	No	No
Structure	Simple	complex	complex	complex
	Arch. V	**Arch. VI**	**Arch. VII**	**Arch. VIII**

the vehicle. The electric power is either stored into ES or reused in EM2 to propel the vehicle after another electro-mechanic conversion. Therefore, EM1 and EM2 create the similar functionality as the planetary gearbox in Toyota Prius and a series-parallel HEV is then realized.

As listed in Table I, four architectures are possible for EM1 regarding to firstly the different connections between its inner rotor (IR) or outer rotor (OR) and EM2 or ICE, and regarding to secondly the different arrangements of PM and windings (W) on two rotors. Architecture **I** and Architecture **III** are finally chosen. The same is done to EM2, and Architecture **V** and Architecture **VIII** are chosen, as seen in Table II.

Merging EM1 and EM2 into an integrated machine is made to achieve a more compact structure. To do that, four possible combinations of Architecture **I, III** and Architecture **V, VIII** can be considered. Although compound structure could also be applied, this paper will only consider such an EVT structure as the one with radial-radial field distribution. Therefore, the combination of Architecture I and Architecture V is chosen for its simple structure, as shown in Fig. 3. In conclusion, the chosen PM-EVT has the following structure:

- an outer stator with windings, which are fed by power electronic converter (PE2 as Fig. 2);

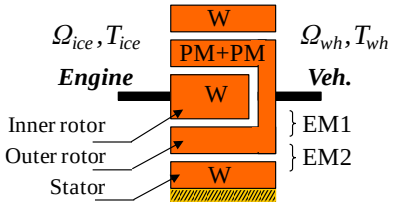

Fig. 3 The chosen PM-EVT structure

- an outer rotor with PMs, which produce the fields in the inner and outer air gaps;
- an inner rotor with windings, which are fed by power electronic converter (PE1 as Fig. 2) through slip ring and brushes.

Although the chosen PM-EVT has the similar structure as [2],[5]-[8], different PM arrangement on the outer rotor is possible. Some of them are shown in Fig. 4. For example, by locating PMs on the surface or in the interior of the outer rotor, as illustrated in Fig.4 (c), the surface-mounted permanent magnet (SMPM) machines or the interior permanent magnet machines (IPM) are achieved. The former has the advantage of simple topology and is widely used for PM brushless machines. The latter exhibits a reluctance torque and a higher inductance, which is appropriate for extended speed operation [14]. Other changes are also possible in order to optimize the machine performance or to simplify its control: to adopt one-layer or multi-layer PMs or radially and tangently magnetized PMs (Fig. 4 (d)), to change the shapes of PMs (Fig. 4 (e)), to adopt various machine types (Fig. 4 (f)), etc.

Because of the simplicity, the structure of SMPM with different pole pairs is chosen for a first PM-EVT in this paper.

III. Definition of EVT Specifications

In order to design a PM-EVT, specifications are defined firstly based on the Toyota Prius II data and simulation [16]. Prius adopts the THS (Toyota Hybrid System), a well-known series-parallel powertrain, to implement its various HEV operation modes. It connects the engine and the driveline by using a planetary gear set and two electric machines.

To make a comparative study, it is assumed that THS system is replaced by EVT (shown in Fig.3) and its input and output speeds and torques are extracted to define EVT specifications. To do that, four different driving cycles are simulated, namely maximum acceleration, highway, urban and road cycle. A steady state model of EVT is considered

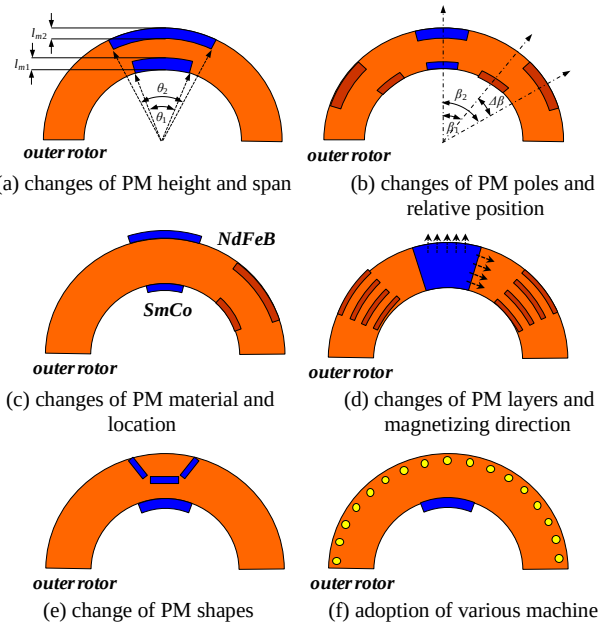

(a) changes of PM height and span
(b) changes of PM poles and relative position
(c) changes of PM material and location
(d) changes of PM layers and magnetizing direction
(e) change of PM shapes
(f) adoption of various machine types

Fig. 4 Different PM arrangement on the outer rotor

for simplicity:

$$\text{EM1}:\begin{cases}\Omega_{em1}=\Omega_{wh}-\Omega_{ice}\\ T_{em1}=T_{ice}\end{cases}$$
$$\text{EM2}:\begin{cases}\Omega_{em2}=\Omega_{wh}\\ T_{em2}=T_{wh}-T_{ice}\end{cases} \quad (1)$$

For EM1, its mission is to realize the speed change and transmit the engine torque T_{ice}. Therefore, its actual speed Ω_{em1} equals to the speed difference of EVT output speed Ω_{wh} and its input speed Ω_{ice}. For EM2, its mission is to realize the torque change. Therefore, its torque T_{em2} equals to the torque difference of EVT output torque T_{wh} and its input torque T_{ice}. In order to achieve the specifications, statistics are made, and the statistics results are listed in Table III.

IV. Machine Design and Preliminary Results

A first PM-EVT has been designed according to the specifications above. Independent design is firstly adopted without considering the magnetic interference between EM1 and EM2. The effect of magnetic interference is also studied later using finite element analysis (FEA) based on Flux2D software.

To design the PM-EVT, main design equations for a normal SMPM are recalled below according to [17]. The electromagnetic torque is expressed as:

$$T = 2\pi r^2 l B_{1g} K_{1s} \quad (2)$$

where r is the rotor radius and l is the rotor length, B_{1g} is the RMS value of the fundamental sinusoidal space component of the air gap flux density created by the magnet, and K_{1s} is the linear current density along the stator periphery. B_{1g} and K_{1s} are limited by many design constraints, including the magnet properties, geometric dimensions, saturation, and cooling capability, etc [17].

The relationship between B_{1g} and the air gap flux density B_g is given by:

$$B_{1g} = \frac{2\sqrt{2}}{\pi} B_g \sin(\alpha) \quad (3)$$

where α is the electrical angle of magnet span ranging 55-80 º. B_g is in the range of 0.85-0.95T.

An empirical equation (4) is used to calculate the minimum air gap g_m above the magnets. Moreover, an arbitrary 5% increase of g_m is assumed to calculate the effective air gap g_e taking the effect of Carters' coefficient into account.

$$g_m \approx 0.0002 + 0.003\sqrt{r \cdot l}\,, \quad g_e = 1.05 g_m \quad (4)$$

TABLE III
Main Specifications of EVT

	EM1		EM2	
	T/Nm	***P/kW***	***T/Nm***	***P/kW***
Long-term operation	110@ 0~2000rpm	23@ 2000~3670 rpm	100@ 0~1900rpm	20@ 1900~6460 rpm
Mid-term operation	110@ 2000~2500 rpm	29@ 2000~3670 rpm	200@ 0~1900rpm	40@ 1900~6460 rpm
Short-term operation	--	--	380@ 0~1450rpm	58@ 1450~6460 rpm

The radial thickness l_m of permanent magnet is defined by:

$$l_m = \frac{\mu_r g_e}{B_r / B_g - 1} \tag{5}$$

where μ_r and B_r are the relative permeability and residual flux density. For NdFeB magnet, $\mu_r \approx 1.05$ and $B_r \approx 1.1$T. When ignoring the leakage flux, one half of the flux in every magnet goes through the yoke. Therefore, the yoke thickness could be expressed as:

$$d_y = \frac{\alpha \cdot r}{p_n} \cdot \frac{B_g}{B_y} \tag{6}$$

where p_n is the number of pole pairs, B_y is the maximum yoke flux density, which is constrained by the core saturation. Typically, B_y is in the range of 1.4~1.7T varying to adjust the core losses.

A slotless PM-EVT is achieved using the equations above, shown in Fig. 5 as well as its field distribution. And the geometric parameters of PM-EVT are listed in Table IV.

By changing the relative position $\Delta\beta$ (mechanical degree) of outer and inner magnets, as Fig.6, FEA simulation is done to study the magnet interference between the EM1 and EM2 machines. When there are only the inner magnets, the magnitude of flux density of the inner air gap B_{in} is 0.831T. And the magnitude of flux density of the outer air gap B_{out} is 0.783T when excited only by the outer magnets.

From Fig. 6, it can be seen that magnetic interference exists between EM1 and EM2 and affects inner and outer air gap fields. B_{in} and B_{out} will change depending on $\Delta\beta$, as Fig.7. When $\Delta\beta$=0, the centers of the outer and inner N-poles are aligned. In this situation, B_{in} and B_{out} become a little higher. It is because that the flux lines produced by inner and outer magnets are subtracted by each other, which makes the majority of flux lines goes through the outer rotor yoke in the radial direction [18]. The flux lines in the tangential direction are much smaller than the situation when excited by only outer or inner magnets, which results in a little higher air gap flux densities.

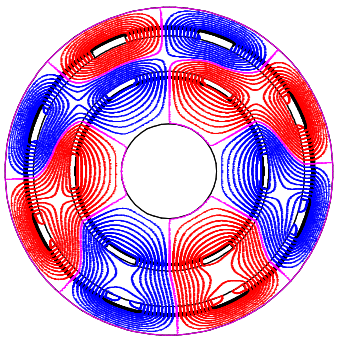

Fig. 5 Field distribution of the slotless PM-EVT

TABLE IV
MAIN PARAMETERS OF PM-EVT

Parameters	Units	Values (EM1)	Values (EM2)
Number of poles	--	6	8
Inner rotor outer radius	mm	78	--
Outer rotor inner radius	mm	84	--
Outer rotor outer radius	mm	--	114
Stator inner radius	mm	--	122
Air gap length	mm	1.5	2
Thickness of magnets	mm	4.5	6
Magnet span (α)	°	120	120
Number of slots per pole per phase	--	1	2
Rated voltage	V	220	220
Resistance per phase	mΩ	222	112
Inductances (L_d=L_q)	mH	2.95	0.91
PM flux linkage	Wb	0.526	0.477

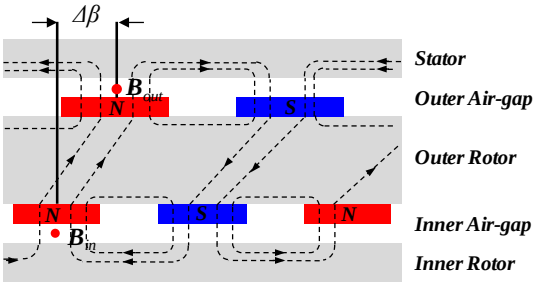

Fig. 6 Relative position change of outer and inner magnets

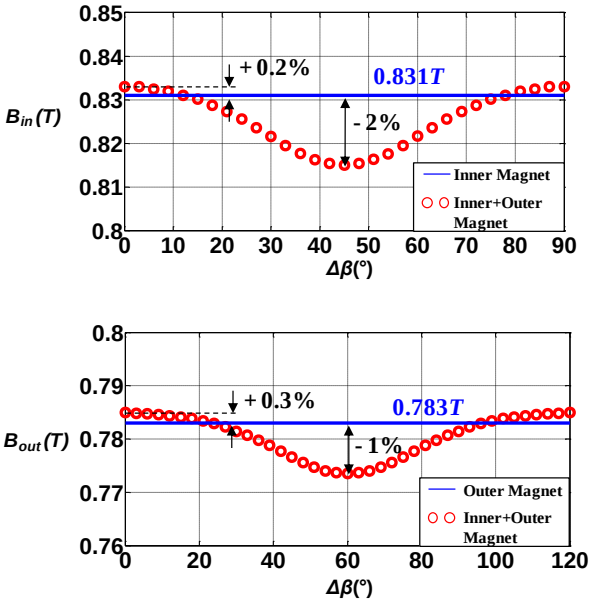

Fig. 7 B_{in} and B_{out} variation with magnet relative position $\Delta\beta$

As $\Delta\beta$ increases, the tangential flux increases more and more, and the outer rotor tends to saturation. When $\Delta\beta$=180 º, B_{in} and B_{out} become the lowest. But since the reduction of the flux densities is less than 2%, we could conclude that, for the preliminary design, the relative position of outer and inner magnets have little effect on the

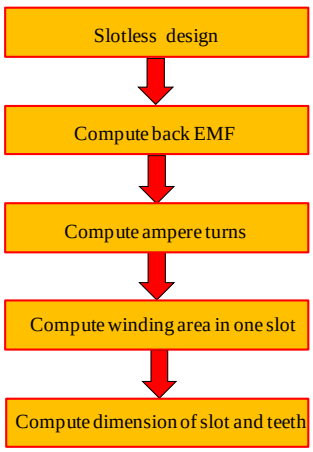

Fig. 8 Design outline of slots and windings

magnetic interference, which could be ignored.

Slots and windings were designed according to the outline in Fig. 8. A slotless design was firstly made by assigning linear current regions along the contour of the stator and the inner rotor. In this way, trapezoid-shaped phase EMF (E_f) could be achieved by rotating its out rotor. Fundamental components e_a, e_b, e_c of phase EMF were extracted to compute the ampere turns (AT) in one slot according to:

$$\begin{aligned} P_{em}(t) &= e_a(t)\cdot i_a(t) + e_b(t)\cdot i_b(t) + e_c(t)\cdot i_c(t) \\ &= 3E_f \cdot AT \cdot \cos(\varphi_e - \varphi_i) \end{aligned} \tag{7}$$

where P_{em} is the required power of the electric machine, i_a, i_b, i_c are the phase currents. i_d=0 control is always adopted to control SMPM under the rated speed, so the EMF and current phases φ_e and φ_i are equal to each other, and the ampere turns are:

$$AT = \frac{P_{em}(t)}{3E_f} \tag{8}$$

with AT, the copper and slot areas S_{copp} and S_{slot} per slot can be calculated as:

$$S_{copp}=AT/J\,, \qquad S_{slot}=S_{copp}/f_s \tag{9}$$

where J is the current density, and fill factor f_s typically ranges from 0.3 to 0.5 [17]. In the first design, the trapezoid-shaped slots are adopted for simplicity. The final geometry of PM-EVT is shown in Fig.9.

The number of turns n_s has a direct effect on the self inductances L_d and L_q, winding resistance R_s, and the induced voltage. It is constrained and calculated according to the voltage limit U_{rms}:

$$\begin{aligned} &L_{d,q} \propto n_s^2\,, \quad R_s \propto n_s^2\,, \; E_f \propto n^s \\ &V^2 = {V_d}^2 + {V_q}^2 = (\omega L_q I_q)^2 + (E_f + I_q R_s)^2 \le U_{rms}^2 \end{aligned} \tag{10}$$

The rated voltage is limited to 220 V, the numbers of turns of EM1 and EM2 are respectively 60 and 48. Finally, the main parameters of the first PM-EVT are listed in Table IV.

V. Conclusion and Future Work

For simplicity, SMPM type PM-EVT was chosen and designed to evaluate the novel hybrid powertrain concept. A whole process was presented to offer an insight into the design of PM-EVT, including its concept, topology choosing, specifications definition, main design equations, and preliminary results. As a first design, the PM-EVT needs more improvement, such as the careful choice of pole pairs, slot and winding design, the validation of power limitations, extended speed operation, etc. Thermal calculation and cooling design are also not included at this step.

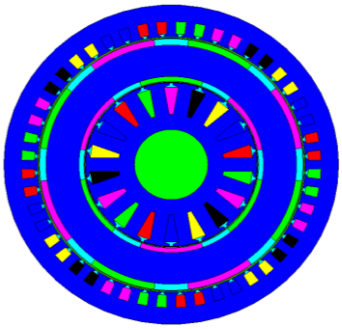

Fig. 9 First design of PM-EVT

References

[1] C.C.Chan. The state of the art of electric, hybrid and fuel cell vehicles. *Proceedings of the IEEE*, Vol.95, No.4, April 2007. 704-718.

[2] M. J. Hoeijmakers, M. Rondel. The electrical variable transmission in a city bus. *Proc. 35th IEEE Power Electron. Specialist Conf.*, 2004, pp. 2773–2778.

[3] M. J. Hoeijmakers, J. A. Ferreira. The electric variable transmission. *IEEE Trans. Ind. Appl.*, vol. 42, n.4, pp. 1092-1093, July/August 2006.

[4] S. Cui, W. Huang, Y. Cheng, K.W. Ning, C.C. Chan. Design and experimental research on induction machine based electrical variable transmission. *Proc. Veh. Power Propulsion Conf.* (*VPPC*), 2007, pp. 231-235.

[5] E. Nordlund and C. Sadarangani, "The four quadrant energy transducer," in Proc. Rec. 37th Conf. IAS Annu. Meeting, 2002, pp. 390-391.

[6] L. Xu, "A new breed of electric machines- basic analysis and applications of dual mechanical port electric machines," in Proc. 8th Int. Conf. Electr. Mach. Syst., 2005, pp. 24–29.

[7] M. Aubertin, A. Tounzi, Y. L. Menach. Study of an electromagnetic gearbox involving two permanent magnet synchronous machines using 3-D-FEM. *IEEE transactions on Magnetics*, Vol. 44, no. 11, November 2008, pp. 4381-4384.

[8] S. Cui, L. Song, S. Han, Y. Cheng, C.C. Chan. "Switched reluctance machine based electromechanical converter with four ports". Chinese invention patent, Application No. 200710072358.5

[9] Karl Hefel. Electric transmission gearing. Patent 461306 (UK), Jan. 1935.

[10] R. Liu, P. Zheng, H. Zhao, C. Sadarangani. Investigation of a compound-structure permanent-magnet synchronous machine used for HEVs. *Proceedings of IEEE Vehicle Power and Propulsion Conference* (*VPPC*), September 2008.

[11] Y. Cheng, "Research on hybrid powertrain based on four ports electromechanical converter," PhD thesis, Harbin Institute of Technology, April 2009 (text in Chinese).

[12] G. Liu, F.Zhang, X. Liu. Performance analysis on opposite-rotation dual mechanical ports PMSM. Proceedings of the International Conference on Electrical Machines and Systems. 2008. pp. 2792-2796.

[13] X. Sun, M. Cheng, W. Hua, L.Xu. Optimal design of double-layer permanent magnet dual mechanical port machine for wind power application. IEEE Trans. Magn., vol.45, n.10, pp. 4613-4616, 2009.

[14] Z.Q. Zhu. Electrical machines and drives for electric, hybrid and fuel cell vehicles. *Proceedings of the IEEE*, Vol.95, No.4, April 2007. 746-765.

[15] K.T. Chau, C.C.Chan, C. Liu. Overview of permanent-magnet brushless drives for electric and hybrid electric vehicles. IEEE Trans. Industrial Electronics, vol.55, n.6, pp. 2246-2257, 2008.

[16] E. Vinot, J. Scordia, R. Trigui, B. Jeanneret, F. Badin (2008) Model simulation, validation and case study of the 2004 THS of Toyota Prius. *International Journal of Vehicle System Modelling and testing*. Vol. 3, No. 3, 2008. pp. 139-167

[17] G.R. Slemon, X. Liu. Modelling and design optimization of permanent magnet motors. Electric Machines and Power Systems, Vol. 20, No.2, March-April 1992, pp. 71-92.

[18] P. Zheng, R. Liu, Q. Wu, J. Zhao, Z. Yao.Magnetic coupling analysis of four-quadrant transducer used for hybrid electric vehicles. *IEEE transactions on Magnetics*, Vol. 43, no. 6, June 2007, pp. 2597-2599.